

NASA TECHNICAL NOTE



NASA TN D-8012 c. /

NASA TN D-8012

2. u/4

LOAN COPY: RET  
AFWL TECHNICAL  
KIRTLAND AFB,



4.  
NUMERICAL STUDY  
OF SOUND PROPAGATION  
IN A JET FLOW

*Sharon L. Padula and Chen-Huei Liu*

*Langley Research Center  
Hampton, Va. 23665*



3.  
NATIONAL AERONAUTICS AND SPACE ADMINISTRATION • WASHINGTON, D. C. • SEPTEMBER 1975



0133886

1. Report No. NASA TN D-8012	2. Government Accession No.		3. Recipient's Catalog No.	
4. Title and Subtitle NUMERICAL STUDY OF SOUND PROPAGATION IN A JET FLOW		5. Report Date September 1975		
		6. Performing Organization Code		
7. Author(s) Sharon L. Padula and Chen-Huei Liu		8. Performing Organization Report No. L-10249		
9. Performing Organization Name and Address NASA Langley Research Center Hampton, Va. 23665		10. Work Unit No. 505-03-12-02		
		11. Contract or Grant No.		
12. Sponsoring Agency Name and Address National Aeronautics and Space Administration Washington, D.C. 20546		13. Type of Report and Period Covered Technical Note		
		14. Sponsoring Agency Code		
15. Supplementary Notes Chen-Huei Liu is an NRC-NASA Resident Research Associate.				
16. Abstract  An improved computer-oriented solution method for problems involving the propagation of sound through a nonuniform jet flow is developed. The method seeks to optimize the use of computer resources such as core storage space and central memory time. Complete formulation details are presented for a jet flow model consisting of a fixed point source on the jet center line in the potential core.				
17. Key Words (Suggested by Author(s)) Sound propagation Jet noise		18. Distribution Statement Unclassified - Unlimited  Subject Category 71		
19. Security Classif. (of this report) Unclassified	20. Security Classif. (of this page) Unclassified	21. No. of Pages 20	22. Price* \$3.25	

# NUMERICAL STUDY OF SOUND PROPAGATION IN A JET FLOW

Sharon L. Padula and Chen-Huei Liu\*  
Langley Research Center

## SUMMARY

An efficient and reliable numerical method for solving problems related to sound propagation through a jet flow field is demonstrated by applying the method to a simple test problem. The test problem is reformulated in terms of a slowly changing variable and a finite-difference approach is employed to solve the resulting elliptic-type partial differential equation. This discretization process yields a system of linear algebraic equations which can be solved by a standard library subroutine with decreased computer time and storage requirements. Comparison of numerical results with those of previous studies and with experimental data demonstrates the improved accuracy of the present analysis.

## INTRODUCTION

Understanding the principles of noise propagation is an essential ingredient of systematic jet noise reduction research. High-speed computer methods offer a unique potential for dealing with complex real life physical systems whereas analytical solutions are restricted to simplified idealized models. The formulation of sound propagation through a jet flow in terms of pressure was found to be impractical for computer solutions and a more suitable approach was needed. Previous investigations by Schubert (ref. 1) and by Liu and Maestrello (ref. 2) selected the phase and amplitude of the acoustic pressure as dependent variables requiring the solution of a system of nonlinear algebraic equations. The nonlinearities complicated both the analysis and the computation. A reformulation of the convective wave equation in terms of a new set of dependent variables was suggested (ref. 3) with a special emphasis on its suitability for numerical solutions on fast computers. The technique is very attractive because the resulting equations are linear in a slowly changing variable. The computer solution to such a linear system of algebraic equations may be obtained by well defined and direct means which conserve computer time and storage space.

In this paper, the reformulation technique is applied to cases equivalent to those presented in reference 1. Complete details of the formulation are contained in the appendix.

---

\*NRC-NASA Resident Research Associate.

Numerical results from the present analysis and from reference 1 are compared with applicable experimental measurements by Grande (ref. 4) and with similar numerical results of Mungur et al. (ref. 5).

## SYMBOLS

A	amplitude of radiated sound wave
c	ambient speed of sound
C	nondimensional $c$ , $c/u_j$
d	jet exit diameter, 0.01905 m
f	frequency
H,K	step sizes, $\Delta\xi$ and $\Delta\eta$ , respectively
M	local flow Mach number, $u/c$
$M_j$	flow Mach number at jet exit, $u_j/c$
n,m	number of grid lines
p	pressure variable
$r, \theta, \phi$	spherical polar coordinates (see fig. 1)
R	nondimensional $r$ , $r/d$
t	time
T	nondimensional $t$ , $tu_j/d$
u	longitudinal component of flow velocity
$u_j$	jet exit velocity
U	nondimensional $u$ , $u/u_j$
x	Cartesian coordinate in windward direction of jet

$X$	nondimensional $x$ , $x/d$
$Z$	complex variable, $AR \exp(i\psi_1)$
$\eta$	coordinate transformation, $\tan^{-1}(\sigma^{-2} \tan \theta)$
$\xi$	coordinate transformation, $\ln R$
$\sigma$	parameter of angular stretching, 0.538 (see eqs. (5))
$\Phi$	velocity-potential variable
$\psi$	phase of radiated sound waves, $\psi_0 + \psi_1/R$
$\psi_0, \psi_1$	components of $\psi$
$\omega$	angular frequency
$\Omega$	nondimensional angular frequency, $\omega d/u_j$

## FORMULATION OF PROBLEM

For illustration purposes, the method developed in this paper is applied to a simple test problem. In a subsequent section, the appropriate convective wave equation is identified and is reformulated for solution. A judicious choice of variables nets a linear partial differential equation which can be efficiently solved by numerical methods.

### The Nonuniform Jet Flow Field

The present method of solution is tested for the case of an acoustic point source located on the center line and contained within the potential core of a spreading jet. (See fig. 1.) The jet nozzle is cylindrical with diameter  $d$ . The jet flow is assumed

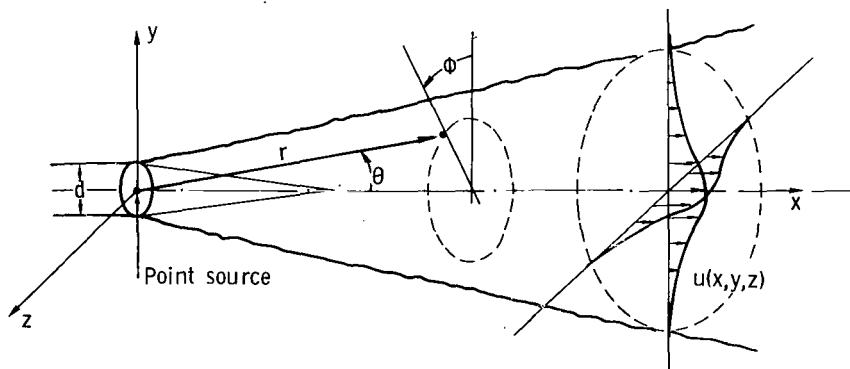


Figure 1.- Jet flow configuration.

unidirectional and axisymmetric but nonuniform and the velocity profiles at any cross section are determined from experimental and empirical data. The origin of the coordinate system is fixed at the source while the origin of the flow-field coordinates is fixed at the virtual origin of the jet. Most of the calculations are done in the spherical polar coordinates  $(r, \theta, \phi)$ .

### The Convective Wave Equation

Sound propagation through a flow field can be described most simply by the following convective wave equation:

$$L(\Phi) = 0 \quad (1)$$

where

$$L = \frac{1}{c^2} \left( \frac{\partial^2}{\partial t^2} + 2u \frac{\partial^2}{\partial x \partial t} + u^2 \frac{\partial^2}{\partial x^2} \right) - \nabla^2$$

is a linear differential operator,  $\Phi$  is Obukhov's "quasi-potential" variable,  $\nabla^2$  is the Laplacian operator in Cartesian coordinates,  $c$  is the ambient speed of sound, and  $u$  is the longitudinal component of flow velocity. A discussion of the use and validity of this formulation can be found in reference 1.

By assuming a harmonic source,  $\Phi$  can be expressed as

$$\Phi = A \exp[i(\psi R - \Omega T)] \quad (2)$$

where  $\Omega = \omega d/u_j$  is the normalized source frequency,  $R = r/d$  is the radial distance from the source,  $T = tu_j/d$  is the time, and  $A$  and  $\psi$  are the amplitude and phase of the radiated sound waves.

Substituting  $\Phi$  into equation (1) results in a time-independent partial differential equation which is nonlinear in  $A$  and  $\psi$ . Schubert (ref. 1) chooses to solve this equation by application of the finite-difference method. This necessitates solving a system of simultaneous nonlinear algebraic equations.

There is no direct method for solving such a system of nonlinear equations. Iterative computer methods are available, but they have a number of drawbacks. First, they are highly specific. The coding is dependent on the problem to be solved and must be rewritten and tested for each new equation. Secondly, the accuracy of the results can be affected by how well and how quickly the process converges. In the case of sound propagation through a flow, it remains to be shown that the process does in fact converge for all instances.

The problems inherent in iterative methods can be avoided by representing the variable  $\psi$  by

$$\psi = \psi_0 + \frac{\psi_1}{R} \quad (3)$$

where  $\psi_1$  is a function of  $r$  and  $\theta$  and  $\psi$  approaches  $\psi_0$  as  $R$  approaches infinity. Then substituting equation (3) into equation (2) gives

$$\Phi = \frac{Z}{R} \exp \left[ i(\psi_0 R - \Omega T) \right] \quad (4)$$

where  $Z$  is a complex variable equal to  $AR \exp(i\psi_1)$ . Equation (1) can be rewritten as a linear partial differential equation in  $Z$ . (See eq. (A2) in the appendix.) In this way, the solution by finite-difference method involves merely the solution of a system of simultaneous linear algebraic equations. Most computer subroutine libraries contain routines adequately suited to this task.

## NUMERICAL SOLUTION

In this section, a solution to the test problem by numerical means is discussed. The techniques employed help to reduce further the computer storage space and central memory time required.

### Underlying Assumptions

The basic assumptions and basic scheme for solving the problem follow directly from previous work. (See refs. 1 and 2.) Details of the formulation can be found in the appendix. Figure 2 shows the spreading jet superimposed on a polar grid. An antijet is assumed in order to avoid problematic boundary conditions along the rigid walls of the jet nozzle.

The value of the complex variable  $Z$  changes most rapidly near the point source and in the region of significant flow. It is desirable to apply the finite-difference method to an unequally spaced grid which has a concentration of points in the areas of greatest change. (See fig. 2.) To avoid the difficulties posed by an uneven grid, an even grid is specified in some new coordinates,  $\xi$  and  $\eta$ . (See fig. 3.) This new grid in  $(\xi, \eta)$  maps onto the desired uneven grid in  $(R, \theta)$  according to the following transformation:

$$\left. \begin{aligned} \xi &= \ln R \\ \eta &= \tan^{-1} (\sigma^{-2} \tan \theta) \end{aligned} \right\} \quad (5)$$

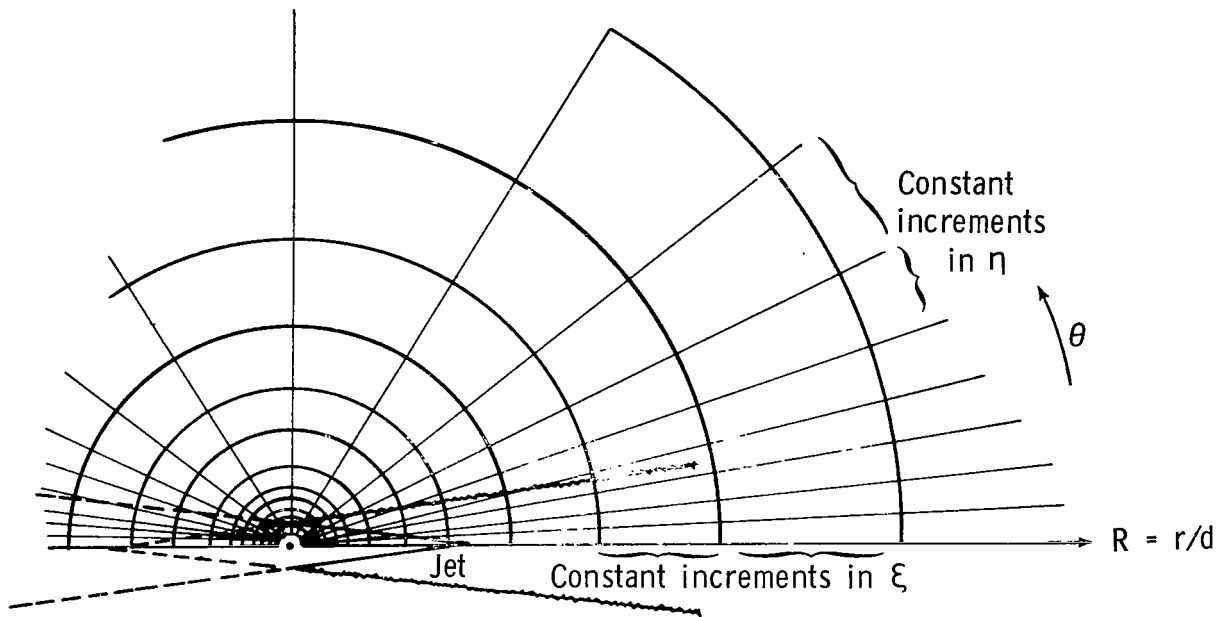


Figure 2.- The finite-difference grid as seen in the physical plane.

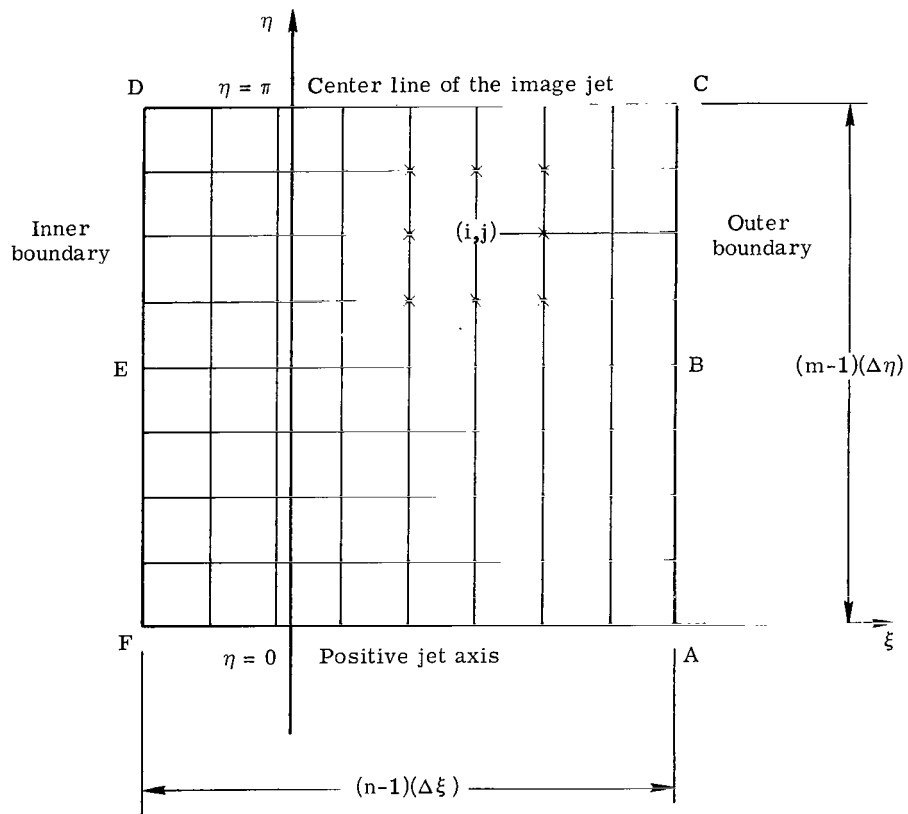


Figure 3.- A grid for the finite-difference method in the  $(\xi, \eta)$  plane.



Here,  $\sigma$  is a parameter ( $\sigma^2 < 1$ ) which determines the amount of angular stretching;  $\sigma = 0.538$  throughout this paper. For illustration purposes, the polar grid in  $(\xi, \eta)$  is thought of as a rectangular grid with  $n \times m$  intersecting lines.

### The Finite-Difference Method

The partial differential equation (1) written in terms of  $Z$  should be satisfied at each interior point of the region of interest. If the partial derivatives in this equation are replaced by their central difference approximations, a nine-point difference equation results. Writing this difference equation at each interior grid point gives  $(n - 2) \times (m - 2)$  equations in  $n \times m$  unknowns. Boundary conditions are the additional equations needed to specify a unique solution.

### Boundary Conditions

The equation in  $Z$  is an elliptic-type partial differential equation, thus, the boundary-value problem is well posed.

The region  $\mathcal{D}$  is bounded by two concentric half circles centered on the point source and by two line segments on the axis of symmetry of the jet. (See fig. 4.) The inner circle has a radius of  $0.25d$  and the outer circle has a radius of  $100d$ , where  $d$  is

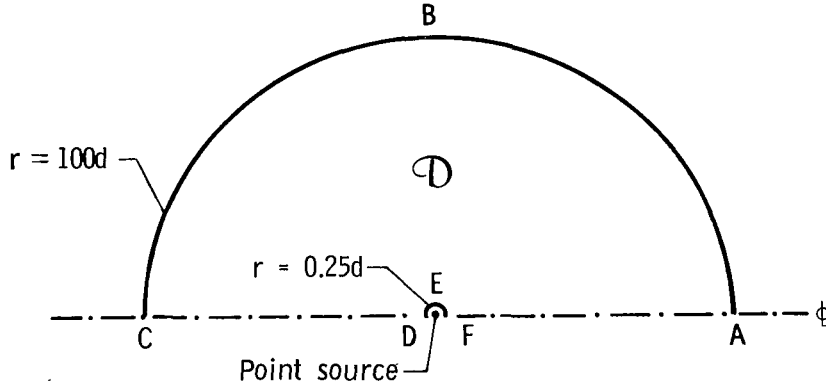


Figure 4.- Domain of the problem.

the diameter of the jet nozzle. In this way, the inner boundary is contained in the potential core of the jet, and the outer boundary approximates the far field.

The inner boundary conditions come from a solution derived by Moretti and Slutsky (ref. 6). The solution is specified for a point source in a uniform flow. It gives the sound pressure level for points a small distance from the source. Since the acoustic source and the inner boundary are contained in the potential core of the jet, they are in a locally uniform flow and the Moretti and Slutsky solution is approximately valid.

The outer boundary conditions at  $100d$  are essentially the far-field radiation conditions. Along the center line, symmetry conditions are imposed in discrete form.

## RESULTS AND DISCUSSION

Numerical results produced by the present analysis are presented in figures 5 to 11. Test cases which demonstrate the utility and reliability of the analysis for a wide range of flow Mach numbers, source frequencies, and radial distances are presented first. The graphs contain either sound pressure level (SPL) or phase information. Comparisons with available experimental data and numerical results follow.

### Test Cases of the Present Analysis

Unless otherwise stated, all test results have been calculated on a grid of  $19 \times 19$  lines, i.e.,  $n = m = 19$ . Figure 5 indicates that for the problem tested a denser grid spacing will cause very little change in the results and reasonable approximate results can be achieved with an  $11 \times 11$  or  $13 \times 13$  grid. Such results can be produced very rapidly in a minimal amount of core storage space.

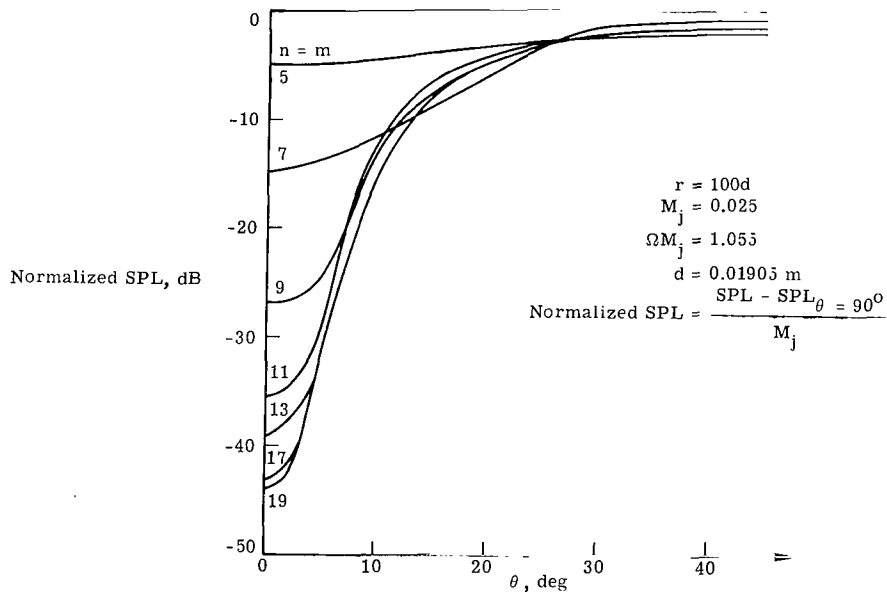


Figure 5.- Effects of the number of grid lines on the solution.

Figure 6 is representative of the numerical results possible with the current approach. Constant sound-pressure-level curves are plotted for a case in which the acoustic point source is located at the intersection of the jet exit plane and the jet center line. Here the flow velocity was Mach 0.3 and the frequency was 3000 Hz.

For the purpose of comparing phase information produced by the present method with that produced by reference 1, results over a range of flow Mach numbers and at three different radial distances from the source are presented in figure 7. Note that in the

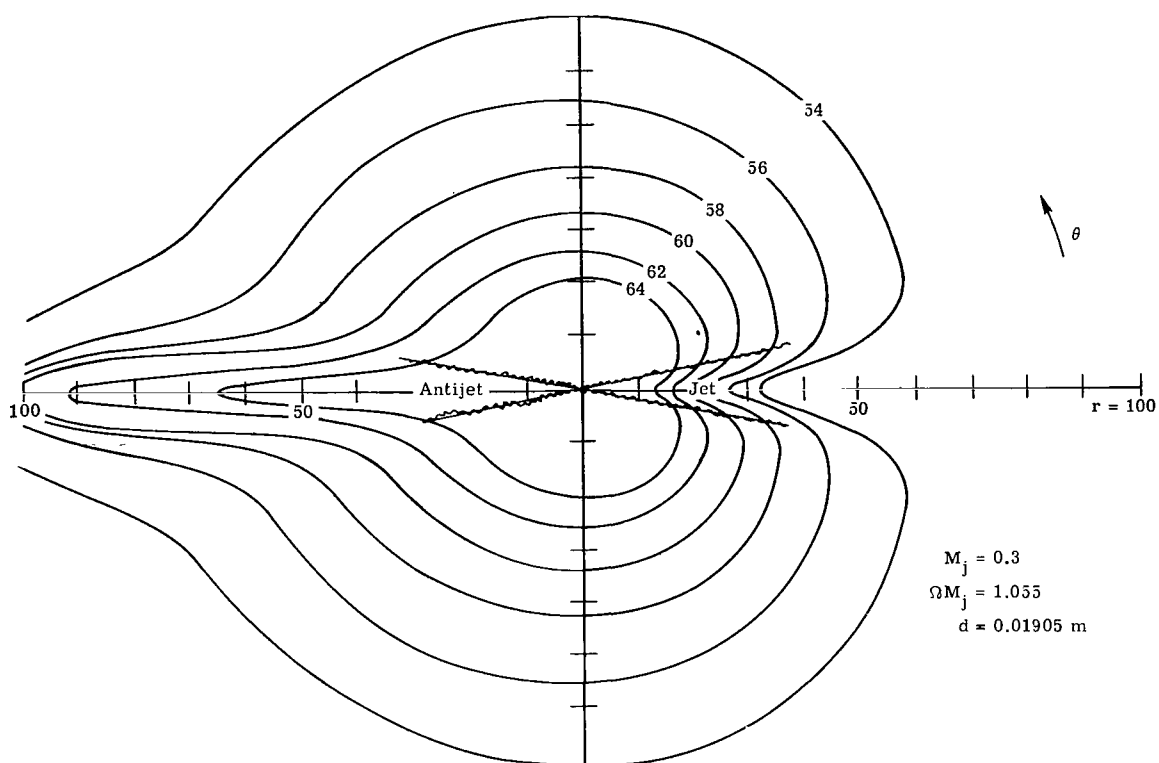


Figure 6.- Sound pressure contours for a point source on the jet exit plane.

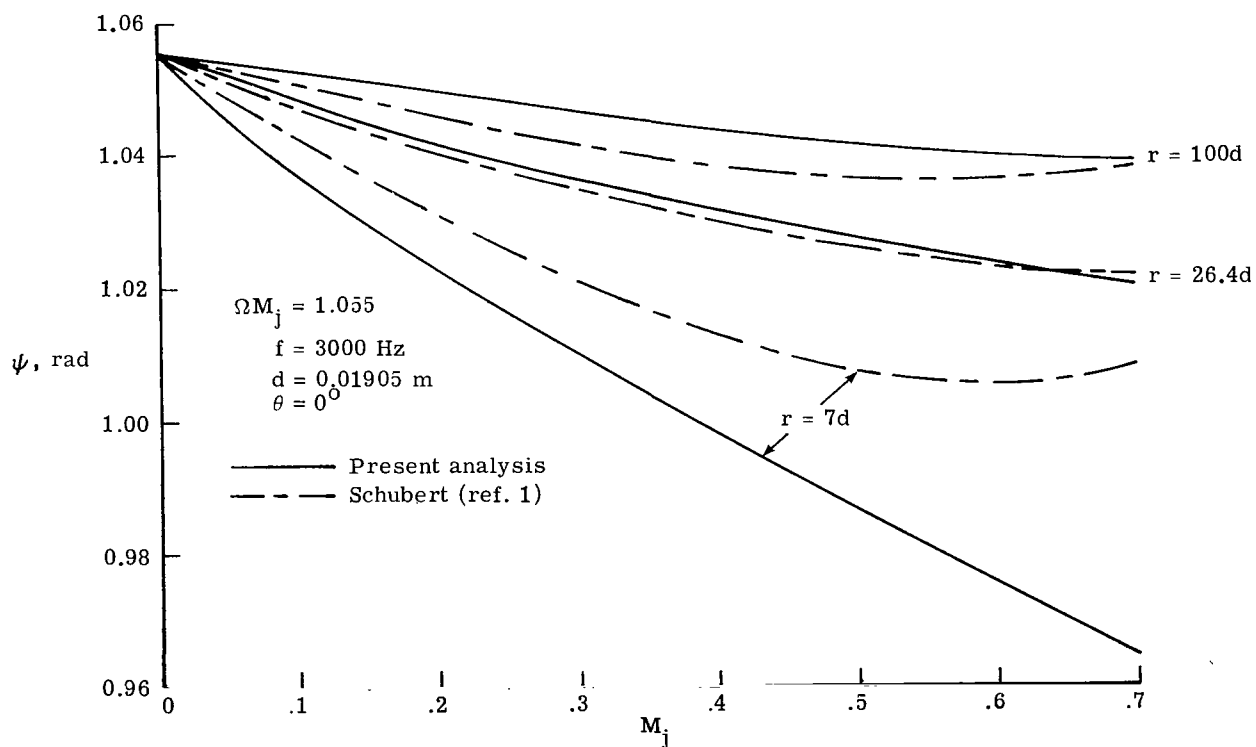


Figure 7.- Phase as a function of Mach number and position.

absence of flow,  $\psi$  equals  $\omega d/c$  for every value of  $r$ . This figure characterizes the differences in results produced by the two methods. Theoretically, the results would be identical, but the different methods have different sources of error. The variation in results is particularly noticeable at small distances from the jet exit.

The results presented herein have been calculated by using a relatively simple formulation for test purposes. The method is in no way restricted to the homogeneous convective wave equation or to the quasi-potential variable  $\Phi$ . Figure 8 illustrates the

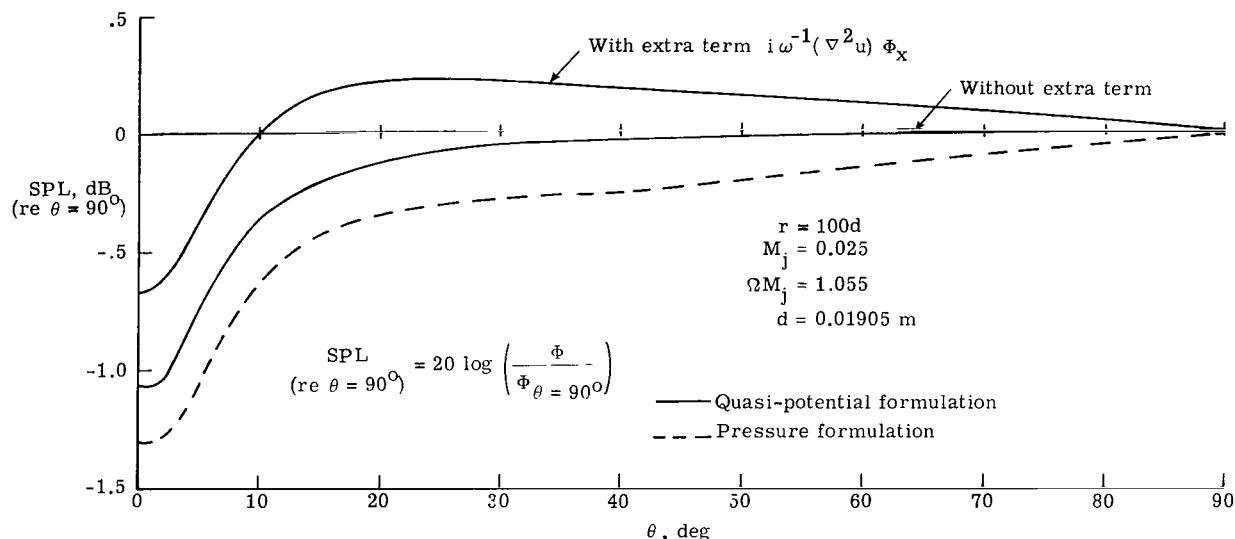


Figure 8.- Comparison of pressure formulation with quasi-potential formulation.

results obtained with two alternate formulations. The label, "quasi-potential formulation with the extra term," refers to the equation which results when a correction term is added to the right-hand side of equation (1). Thus,

$$L(\Phi) = \frac{i}{\omega} (\nabla^2 u) \frac{\partial \Phi}{\partial x} \quad (6)$$

Pressure formulation implies use of the equation  $L(p) = 0$  with the proper pressure information specified on the inner boundary. (See refs. 1, 2, and 6.) The comparison of pressure formulation with the two quasi-potential formulations were calculated at a flow Mach number of 0.025. Relative sound pressure level is plotted against  $\theta$ . For this low flow case, the results are very much alike.

### Comparison of Numerical and Experimental Results

Figure 9 is presented to illustrate the success of the current analysis for problems over a wide range of frequencies and flow Mach numbers. Numerical results from reference 1 and experimental data of reference 4 are plotted as well as the numerical results

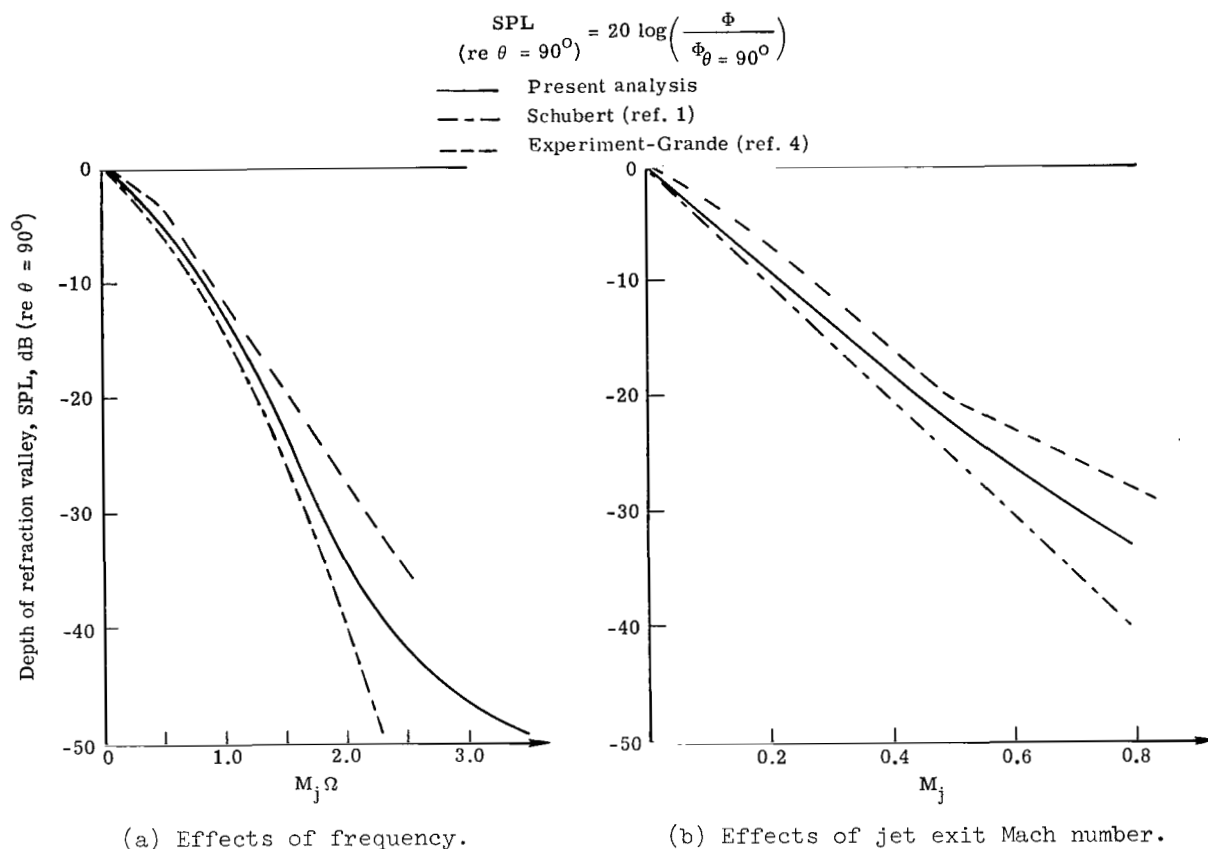


Figure 9.- Sound pressure level at  $r = 100d$  and  $\theta = 0^\circ$ .

of the present method. Sound pressure level on the jet center line relative to SPL at  $\theta = 90^\circ$  is plotted against nondimensionalized frequency in figure 9(a) and against flow Mach number in figure 9(b). It is evident that the current analysis is in agreement with experimental findings. Moreover, the current method produces results which are even closer to experimental values than the results of reference 1.

Providing more detailed information, the next two figures (figs. 10 and 11) show sample results at several flow velocities and acoustic source frequencies. In each graph, sound pressure level relative to SPL at  $\theta = 90^\circ$  is plotted against  $\theta$ . These figures allow comparisons of the results of this paper with experimental data of reference 4 and the numerical results of reference 1.

Figure 10 shows comparable results for the flow velocities Mach 0.3, Mach 0.5, and Mach 0.9. The radial distance from the source and the source frequency are 100d and 3000 Hz, respectively, in each of the three graphs. Notice that the correspondence between experimental data and the current numerical results is especially good at the lower Mach numbers. Also, notice the discrepancies between the numerical results of reference 1 and experimental results at these same Mach numbers.

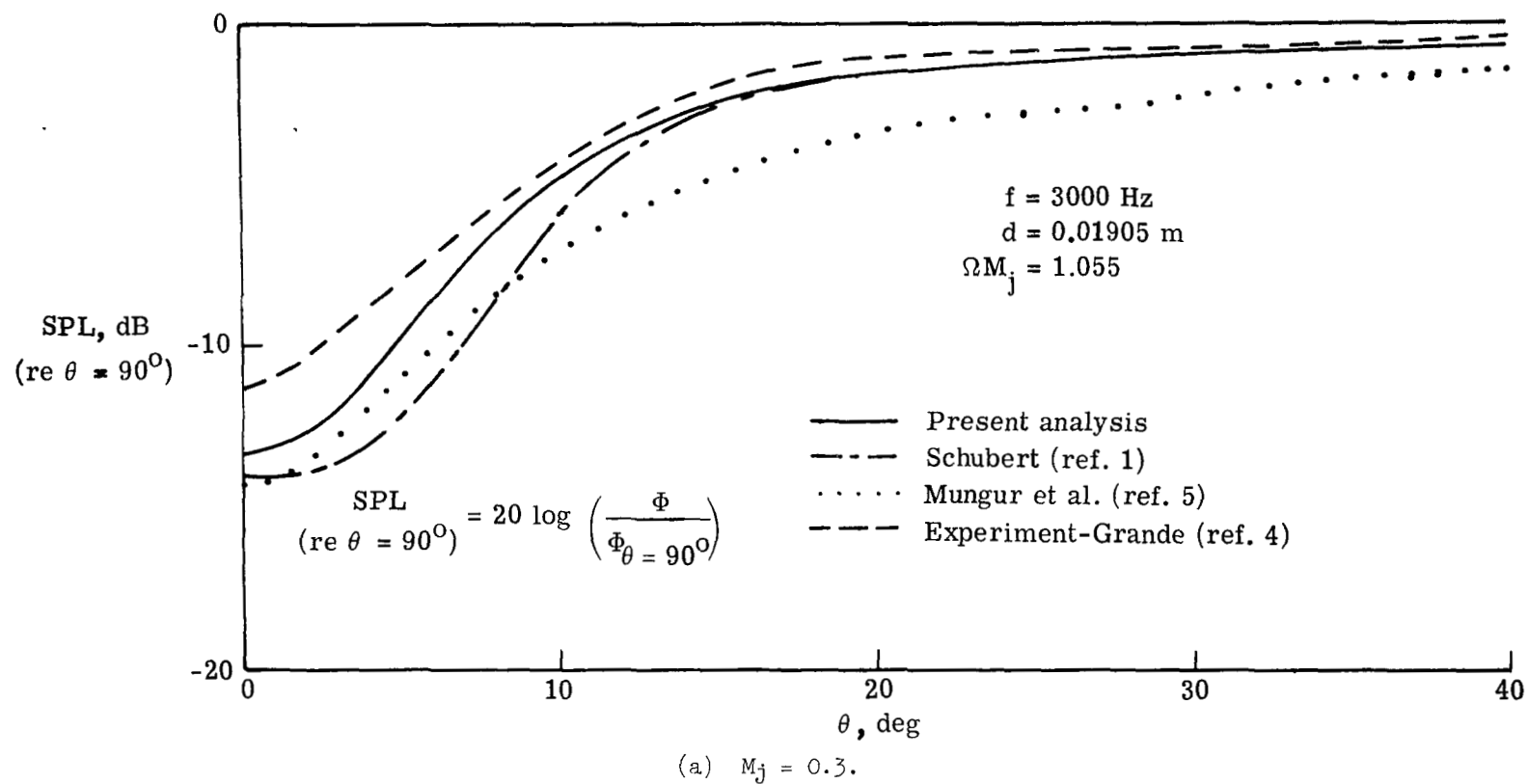
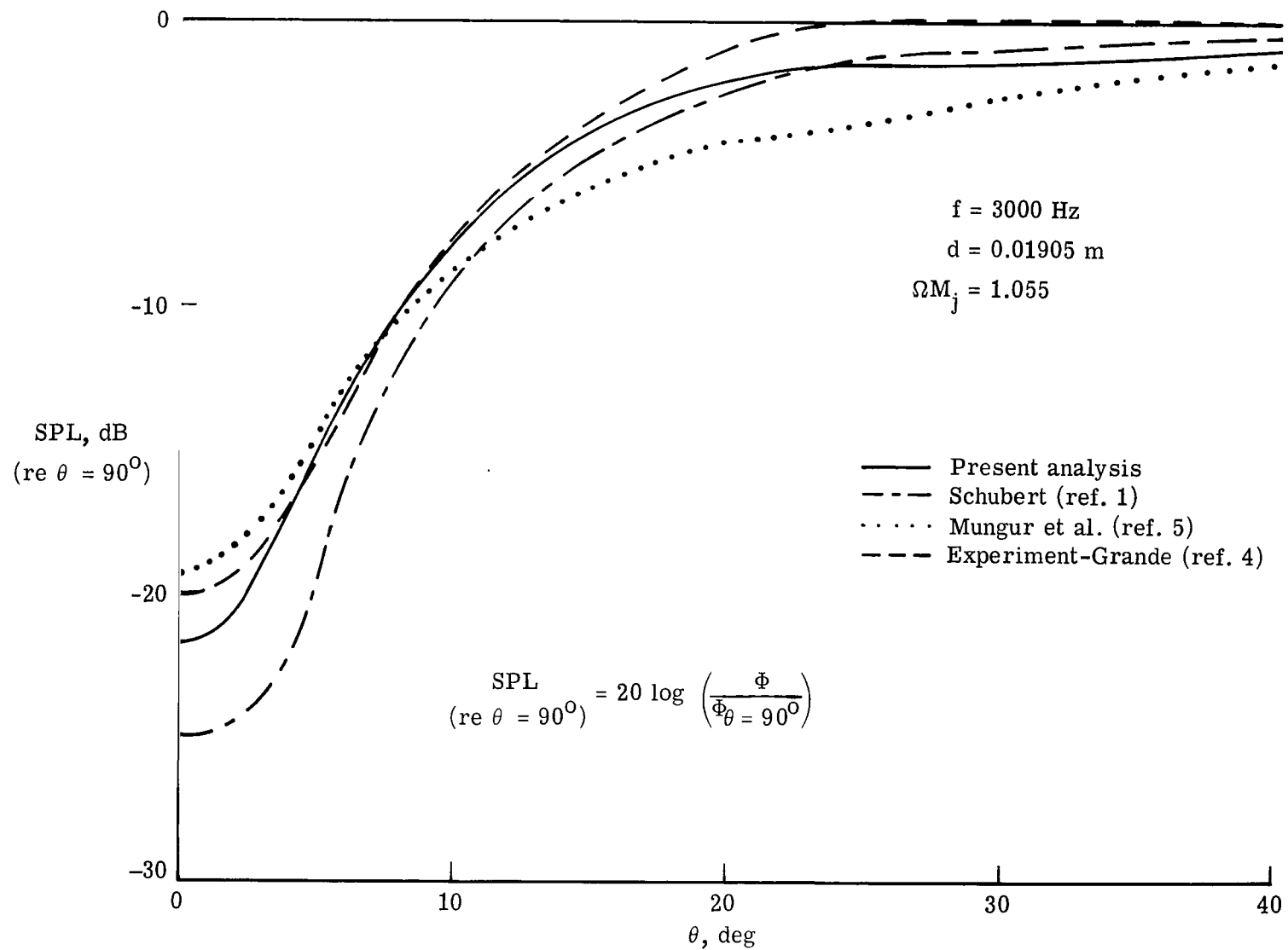
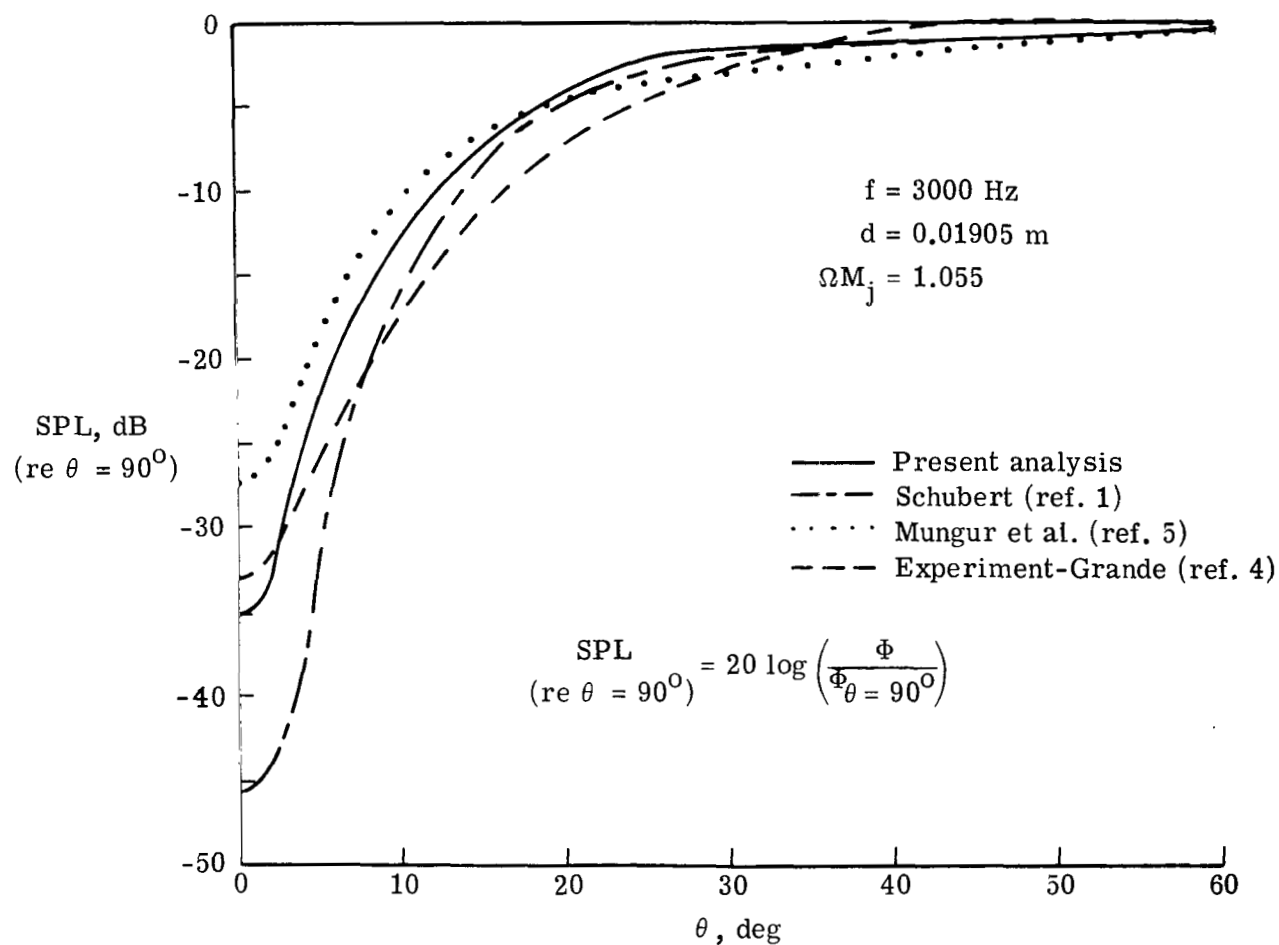


Figure 10.- Effects of jet exit Mach number on sound pressure level at  $r = 100d$ . Source at  $2d$ .



(b)  $M_j = 0.5$ .

Figure 10.- Continued.



(c)  $M_j = 0.9$ .

Figure 10.- Concluded.



Numerical results of reference 5 are also presented in figure 10 for interest. Both the mathematical approach and the jet flow model used in reference 5 are significantly different from those of the current work. Thus, a fair comparison of one method with the other is not possible.

The radial distance and flow velocity are constant ( $r = 100d$  and  $M_j = 0.3$ ) in figure 11, while the frequency changes from 3000 to 5000 to 7000 Hz. In all cases, numerical results obtained by the present method represent an improvement over those obtained in reference 1 with respect to their agreement with experiment.

— Present analysis  
 - - - Schubert (ref. 1)  
 - - - Experiment-Grande (ref. 4)

$$M_j = 0.3$$

$$d = 0.01905 \text{ m}$$

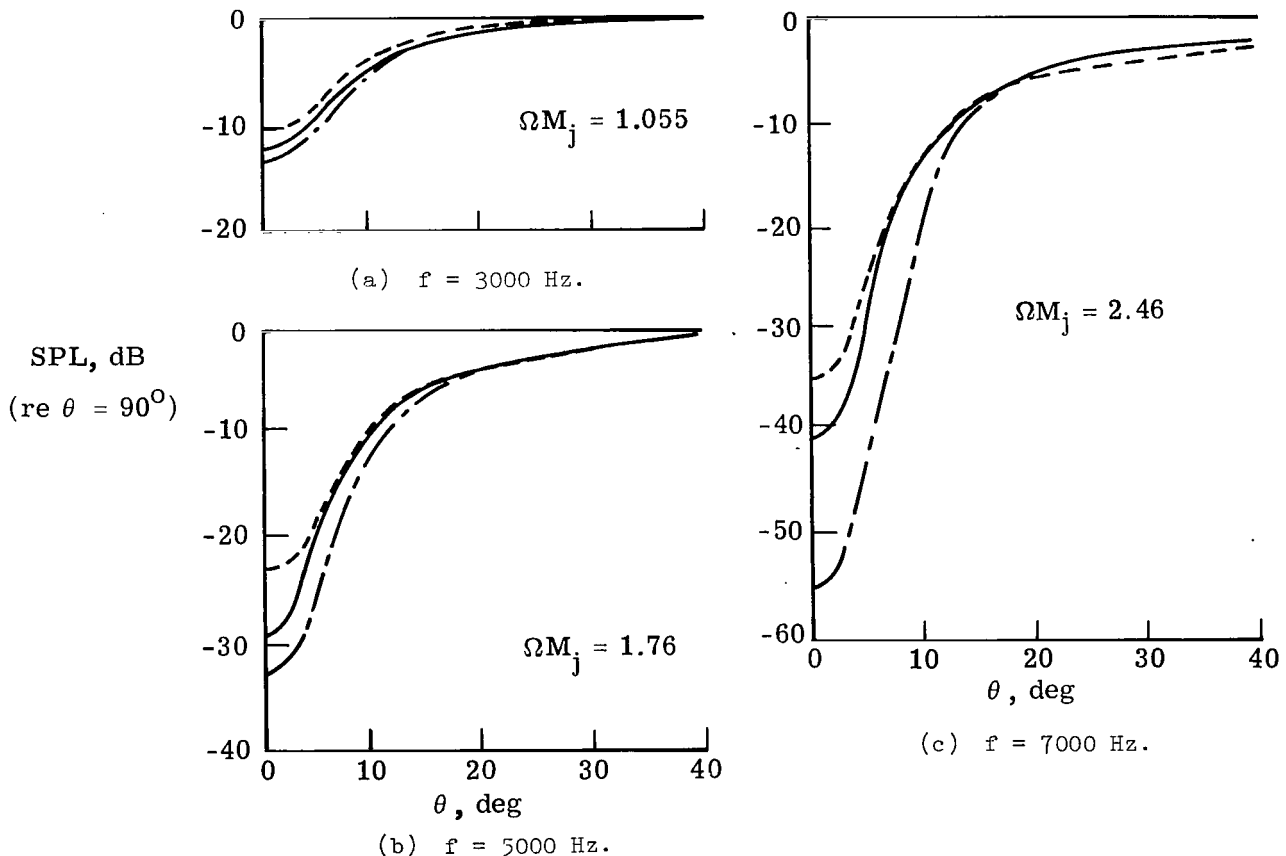


Figure 11.- Effects of frequency on sound pressure level at  $r = 100d$ . Source at  $2d$ .

### Advantages of the Method

It should be emphasized that the present method and the method of reference 1 use the same sound propagation model for testing purposes. Theoretically, they should produce identical results. Differences arise when theory is translated into practical computer programs. Iterative methods, such as the one described in reference 1, are often inaccurate because the iterative process must be terminated after a reasonable amount of computer time has elapsed. Furthermore, an iterative method is more susceptible to round-off errors which tend to multiply as computing time increases. Direct methods, such as the method presented herein, largely avoid these problems and generally produce more reliable results.

The present method has other advantages besides accuracy. It is quite straightforward and relatively easy to program. A typical program will execute in well under 1 min of central memory time in a Control Data 6600 computer system. The computer storage space requirements are reasonable so that transfer of data to and from peripheral storage devices is unnecessary.

### CONCLUDING REMARKS

Application of the method presented herein to the solution of sound propagation problems has distinct advantages in that formulation of the problem in terms of a single slowly changing variable reduces the finite-difference approximation to a system of linear algebraic equations. This system may then be solved by a standard library subroutine to give results which are accurate and yet economical to generate. Comparison with previous analysis and experimental data reveals that the present method yields more reliable results with decreased computer requirements. Finally, since the method is versatile and the programming task is relatively uncomplicated, the technique is a promising tool for future sound propagation studies.

Langley Research Center  
National Aeronautics and Space Administration  
Hampton, Va. 23665  
June 26, 1975

## APPENDIX

### FORMULATION OF NUMERICAL SOLUTION

The following steps were used to transform equation (1) for solution by numerical methods. First, equation (1) can be written in terms of nondimensional variables

$$C^{-2}(\Phi_{TT} + 2U\Phi_{XT} + U^2\Phi_{XX}) - \Delta\Phi = 0 \quad (A1)$$

where  $T = tu_j/d$ ,  $C = c/u_j$ ,  $X = x/d$ ,  $U = u/u_j$ , and  $\Delta$  is the normalized Laplacian operator.

A transformation to spherical polar coordinates  $(R, \theta, \phi)$  causes the following changes in equation (A1):

$$\begin{aligned} \frac{\partial^2}{\partial X \partial T} &= \cos \theta \frac{\partial^2}{\partial T \partial R} - R^{-1} \sin \theta \frac{\partial^2}{\partial T \partial \theta} \\ \frac{\partial^2}{\partial X^2} &= \cos^2 \theta \frac{\partial^2}{\partial R^2} - R^{-1} \sin 2\theta \frac{\partial^2}{\partial R \partial \theta} + R^{-2} \sin^2 \theta \frac{\partial^2}{\partial \theta^2} \\ &\quad + R^{-1} \sin^2 \theta \frac{\partial}{\partial R} + R^{-2} \sin 2\theta \frac{\partial}{\partial \theta} \end{aligned}$$

Furthermore, since it has been assumed that the jet is axisymmetric,  $\Phi_{\phi\phi} = 0$  and the Laplacian operator  $\Delta$  in spherical polar coordinates is defined by

$$\Delta = \frac{\partial^2}{\partial R^2} + \frac{2}{R} \frac{\partial}{\partial R} + \frac{1}{R^2} \frac{\partial^2}{\partial \theta^2} + \frac{\cot \theta}{R^2} \frac{\partial}{\partial \theta}$$

Now, using equation (4) to specify  $\Phi$ , equation (A1) may be rewritten as

$$\sum_{K=0}^2 \sum_{L=0}^K \alpha_{K,L}(R, \theta) \frac{\partial^{(K)} Z}{\partial R^{(K-L)} \partial \theta^{(L)}} = 0 \quad (A2)$$

where

$$\begin{aligned} \alpha_{0,0} &= \frac{1}{R} \left[ (M_j \Omega - M \psi_0 \cos \theta)^2 + \frac{M^2}{R^2} (1 - 3 \cos^2 \theta) - \psi_0^2 \right] \\ &\quad - i \left( \frac{1}{R^2} \right) [2MM_j \Omega \cos \theta + M^2 (1 - 3 \cos^2 \theta) \psi_0] \end{aligned}$$

# APPENDIX

$$\alpha_{1,0} = -\frac{M^2}{R^2}(1 - 3 \cos^2 \theta) + i\left(\frac{2}{R}\right)\left[MM_j\Omega \cos \theta + (1 - M^2 \cos^2 \theta)\psi_0\right]$$

$$\alpha_{1,1} = \frac{\cot \theta}{R^3}(1 - 4M^2 \sin^2 \theta) - i\left(\frac{2M \sin \theta}{R^2}\right)(M_j\Omega - M\psi_0 \cos \theta)$$

$$\alpha_{2,0} = \frac{1}{R}(1 - M^2 \cos^2 \theta)$$

$$\alpha_{2,1} = \frac{1}{R^2} M^2 \sin 2\theta$$

$$\alpha_{2,2} = \frac{1}{R^3}(1 - M^2 \sin^2 \theta)$$

The transformation into the  $(\xi, \eta)$  coordinate system is defined by equation (5). When applied to equation (A2) this transformation yields

$$\sum_{\kappa=0}^2 \sum_{\iota=0}^{\kappa} \beta_{\kappa, \iota} \frac{\partial^{(\kappa)} Z}{\partial \xi^{(\kappa-\iota)} \partial \eta^{(\iota)}} = 0 \quad (\text{A3})$$

where

$$\beta_{0,0} = \alpha_{0,0}$$

$$\beta_{1,0} = R^{-1}(\alpha_{1,0} - R^{-1}\alpha_{2,0})$$

$$\beta_{1,1} = B_1(\alpha_{1,1} + B_2\alpha_{2,2})$$

$$\beta_{2,0} = R^{-2}\alpha_{2,0}$$

$$\beta_{2,1} = R^{-1}B_1\alpha_{2,1}$$

$$\beta_{2,2} = B_1^2\alpha_{2,2}$$

and where

$$B_1 = \frac{\sigma^2 \sec^2 \theta}{\sigma^4 + \tan^2 \theta}$$

$$B_2 = \frac{2 \tan \theta (\sigma^4 - 1)}{\sigma^4 + \tan^2 \theta}$$

## APPENDIX

Finally, the set of difference equations on an  $(n - 2) \times (m - 2)$  grid of the interior region of interest may be written

$$\sum_{\kappa, \ell=1}^3 \gamma_{\kappa, \ell} Z_{i+\ell-2, j-\kappa+2} = 0 \quad \left\{ \begin{array}{l} (i = 2, 3, \dots, n - 1) \\ (j = 2, 3, \dots, m - 1) \end{array} \right. \quad (\text{A4})$$

where  $[\gamma_{\kappa, \ell}]$  can be defined as the  $3 \times 3$  matrix

$$\begin{bmatrix} -\frac{\beta_{2,1}}{4HK} & \frac{\beta_{1,1}}{2K} + \frac{\beta_{2,1}}{K^2} & \frac{\beta_{2,1}}{4HK} \\ -\frac{\beta_{1,2}}{2H} + \frac{\beta_{2,0}}{H^2} & \beta_{0,0} - \frac{2\beta_{2,2}}{K^2} - \frac{2\beta_{2,0}}{H^2} & \frac{\beta_{1,0}}{2H} + \frac{\beta_{2,0}}{H^2} \\ \frac{\beta_{2,1}}{4HK} & -\frac{\beta_{1,1}}{2K} + \frac{\beta_{2,2}}{K^2} & -\frac{\beta_{2,1}}{4HK} \end{bmatrix}$$

and where  $H = \Delta\xi$  and  $K = \Delta\eta$ .

The additional equations needed to solve this system uniquely are the boundary conditions which follow. The inner boundary conditions are simply stated

$$Z_{1,j} = (AR)_{1,j} \quad (j = 1, 2, \dots, m) \quad (\text{A5})$$

Likewise, the discrete outer boundary conditions (refs. 1 and 2) are

$$Z_{n,j} = \left(\frac{4}{2+H}\right)Z_{n-1,j} - \left(\frac{2-H}{2+H}\right)Z_{n-2,j} \quad (j = 2, 3, \dots, m - 1) \quad (\text{A6})$$

Lastly, the three-point symmetry conditions on the jet center line can be written

$$\left. \begin{array}{l} Z_{i,1} = \frac{4}{3} Z_{i,2} - \frac{1}{3} Z_{i,3} \\ Z_{i,m} = \frac{4}{3} Z_{i,m-1} - \frac{1}{3} Z_{i,m-2} \end{array} \right\} \quad (i = 2, 3, \dots, n) \quad (\text{A7})$$

## REFERENCES

1. Schubert, L. K.: Numerical Study of Sound Refraction by a Jet Flow. II. Wave Acoustics. J. Acoust. Soc. America, vol. 51, no. 2, pt. 1, Feb. 1972, pp. 447-463.
2. Liu, C. H.; and Maestrello, L.: Propagation of Sound Through a Real Jet Flowfield. AIAA Paper No. 74-5, Feb. 1974.
3. Padula, Sharon L.; and Liu, C. H.: A Computing Method for Sound Propagation Through a Nonuniform Jet Stream. NASA TM X-71941, 1974.
4. Grande, E.: Refraction of Sound by Jet Flow and Jet Temperature - Extension of Temperature Range Parameters and Development of Theory. NASA CR-840, 1967.
5. Mungur, P.; Plumblee, H. E.; and Doak, P. E.: Analysis of Acoustic Radiation in a Jet Flow Environment. J. Sound & Vib., vol. 36, no. 1, Sept. 8, 1974, pp. 21-52.
6. Moretti, Gino; and Slutsky, Simon: The Noise Field of a Subsonic Jet. AFOSR TN-59-1310, U.S. Air Force, Nov. 1959.



812 001 C1 U H 750808 S00903DS  
DEPT OF THE AIR FORCE  
AF WEAPONS LABORATORY  
ATTN: TECHNICAL LIBRARY (SUL)  
KIRTLAND AFB NM 87117

POSTMASTER: If Undeliverable (Section 158  
Postal Manual) Do Not Return

*"The aeronautical and space activities of the United States shall be conducted so as to contribute . . . to the expansion of human knowledge of phenomena in the atmosphere and space. The Administration shall provide for the widest practicable and appropriate dissemination of information concerning its activities and the results thereof."*

—NATIONAL AERONAUTICS AND SPACE ACT OF 1958

## NASA SCIENTIFIC AND TECHNICAL PUBLICATIONS

**TECHNICAL REPORTS:** Scientific and technical information considered important, complete, and a lasting contribution to existing knowledge.

**TECHNICAL NOTES:** Information less broad in scope but nevertheless of importance as a contribution to existing knowledge.

**TECHNICAL MEMORANDUMS:** Information receiving limited distribution because of preliminary data, security classification, or other reasons. Also includes conference proceedings with either limited or unlimited distribution.

**CONTRACTOR REPORTS:** Scientific and technical information generated under a NASA contract or grant and considered an important contribution to existing knowledge.

**TECHNICAL TRANSLATIONS:** Information published in a foreign language considered to merit NASA distribution in English.

**SPECIAL PUBLICATIONS:** Information derived from or of value to NASA activities. Publications include final reports of major projects, monographs, data compilations, handbooks, sourcebooks, and special bibliographies.

**TECHNOLOGY UTILIZATION PUBLICATIONS:** Information on technology used by NASA that may be of particular interest in commercial and other non-aerospace applications. Publications include Tech Briefs, Technology Utilization Reports and Technology Surveys.

*Details on the availability of these publications may be obtained from:*

**SCIENTIFIC AND TECHNICAL INFORMATION OFFICE**

**NATIONAL AERONAUTICS AND SPACE ADMINISTRATION**

**Washington, D.C. 20546**